COMPARISON OF UAV IMAGE SPATIAL RESOLUTION BASED ON THE SIEMENS STAR TARGET

S. A. Fakhri [1] *, S. Motayyeb [2], M. Saadatseresht [2], H. Zakeri [3], V. Mousavi [4]

[1] Dept. of Geomatic Engineering, Faculty of Civil Engineering and Transportation, University of Isfahan, Isfahan, Iran - aryafakhri@trn.ui.ac.ir

[2] Dept. of Photogrammetry and Remote Sensing, School of Surveying and Geospatial Engineering, University College of Engineering, University of Tehran, Tehran, Iran – soroush.motayyeb@ut.ac.ir, msaadat@ut.ac.ir

[3] Department of Civil and Environmental Engineering, Amirkabir University of Technology, Tehran, Iran – h-zakeri@aut.ac.ir

[4] Geomatics Engineering Faculty, K.N. Toosi University of Technology, Tehran, Iran - vmoosavy@mail.kntu.ac.ir

KEY WORDS: UAVs, Spatial Resolution, Siemens Star Target, Ground Resolved Distance, Ground Sampling Distance, Point Spread Function.

ABSTRACT:

In recent years, as the use of Unmanned Aerial Vehicle (UAV) imaging systems has increased, the photogrammetry community has conducted extensive research on the unique advantages of these systems. The UAVs are considered as one of the most important platforms for photogrammetry applications from various urban and non-urban areas at different scales. In UAV photogrammetry projects the spatial resolution of the images must be determined prior to the imaging stage. The spatial resolution of the images is a commonly-used criterion for detecting the smallest distance between two adjacent separable objects in the images. Numerous methods have been developed to precisely evaluate the spatial resolution of images. In this study, the Siemens star target, which is one of the most commonly used artificial targets for analysing spatial resolution was studied. The objective of this paper is to evaluate and compare the reduction of spatial resolution coefficient using the Siemens star target in images captured by UAVs. To this end, a method for automatically detecting the radius of the circle of ambiguity and calculating spatial resolution in UAV images has been developed. According to the findings of this study, the initial step in creating the Siemens star target, in terms of size and the number of acceptable arms, is dependent on the flying altitude of the UAV and the level of image blur. In addition, the reduction in spatial resolution of images captured by various UAVs varies, and its coefficient must be calculated for each project.

1. INTRODUCTION

Unmanned aerial vehicle (UAV) photogrammetry systems have been considered as a highly efficient and valuable mapping tool due to their ability to capture images from non-metric cameras and generate maps and spatial data. These systems consist of ground stations, flying platform, non-metric cameras, guidance software, GPS/IMU, and data processing and production software (Yang, 2021; Yu, 2022). Today With the advancement of UAV technology and its capabilities, new applications such as land monitoring (Cryderman, 2014; Park, 2021), construction projects (Fakhri, 2019; Fakhri, 2022), monitoring forest and natural resource management (Fakhri, 2021; Kangas, 2018) and bridge inspection (Mohammadi, 2021) are being evolved.

Automatic Arial Triangulation (AAT) is conducted as a standard technique in UAV photogrammetry which is performed through tie points extraction (Mousavi, 2021a). The quality of selected tie points is an important and influential factor in the accuracy and quality of products generated using UAV photogrammetry (Mousavi, 2021b). To accurately extract an adequate number of tie points, it is necessary to design an imaging network before concluding photogrammetry operations with UAVs (Saadatseresht, 2015).

The imaging network design includes determining Ground Sampling Distance (GSD) based on the scale of the map or the accuracy of the required spatial information, as well as the spatial resolution of the camera images used. Based on these information, the flight lines are designed based on the shape and dimensions of the mapping area with respect to the required side-lap and flight altitude on different flight lines considering the focal length of the camera and changes in flying altitude. In addition, designing cross flight lines and estimating image motion due to the speed of the UAVs are required to achieve accurate results. UAV cameras are low cast, lightweight, and provide adequate spatial resolution. However, the lens distortions in non-metric cameras used by UAV platforms result in lower image resolution than the pre-designed GSD which negatively affects the precise 3D modelling (Motayyeb, 2022). Therefore, the spatial resolution of the camera is defined to explain the quality of geometric resolution and the detection of object detail using the Ground Resolved Distance (GRD) criterion which is directly related to the GSD. In addition, image spatial resolution is affected by lens resolution, platform vibration, linear and rotational image motion, inability to see due to dust, smoke, and fog, light conditions affecting image brightness and contrast, and conditions for scattering phenomenon due to wave light physics (when the aperture or pixel size of the sensor is too small). As a result, these elements are modelled as a coefficient k in the equation $GRD = k \times GSD$. Because flight altitude design is based on GSD, the technical report and spatial information for the mapping operation must contain an accurate estimation of k. The flight altitude design employs the equation $H = f / ps \times GSD$, where f is the focal length of the lens, ps is the sensor pixel size and GSD is the ground pixel size which is calculated by $GSD = GRD/k$, where GRD is extracted with respect to the map scale using the instructions. To prepare a map with a scale of 1:500, 1:1000 or 1:2000, the GRD value should equal 8% of the map's scale,

---

which is equivalent to 4,8 and 16 cm with a 25% decrease or increase. As a result, the requested map scale leads to the determination of GRD, and with k, the value of GSD is calculated, and with it, f, and ps, the value of flying altitude H is designed (Fakhri, 2021). In addition, because the resolution of the lens may vary between imaging projects, it is necessary to use a spatial resolution test target (Siemens star or bar) that is appropriate for the camera's specifications, flight altitude, area coverage, and GSD imaging. There are typically two methods for measuring spatial resolution parameters: laboratory and field methods. Laboratory procedures cannot be utilized in any circumstance or at any time. Consequently, field methods are the most prevalent technique for measuring spatial resolution parameters. In this regard, field methods can be divided into two broad categories: the use of targets with a particular geometric shape and the use of natural objects in images (Azimi, 2013). Consequently, the following are a few examples of how geometrically targeted targets can be utilized:

Azimi et al. (2013) determined the spatial resolution of Ultra Cam-d images using a Siemens star. General steps of their method include forming circular profiles to the centre of the Siemens star target, estimating the discrete contrast function, and estimating the spatial resolution of the camera. According to the results, the measured spatial resolution is slightly lower than the nominal value (Azimi, 2013).

Using images captured by fixed-wing and multi-rotor UAVs, Lee et al. (2016) determined the spatial resolution of images. They captured images of the Siemens star target from a height of 260 meters using a Canon IXUS 127 HS camera mounted on a fixed-wing UAV, and from a height of 130 meters using a Sony NEX-5N camera mounted on a multi-rotor UAV. The GSD obtained with a fixed-wing UAV at 130 and 260 meters was 4.08 and 7.94, respectively, and the value obtained at 130 meters was calculated to be 4.10. They concluded, first, that determining the spatial resolution of orthophoto images obtained by UAVs at different altitudes is consistent with theory, and second, that the spatial resolution at fixed altitudes for both fixed-wing and multi-rotor UAVs is nearly identical, with the only difference of image colors (Lee, 2016).

According to Lee et al. (2019), determining the spatial resolution is one of the most essential criteria for assessing the quality of UAV images. To evaluate the image quality of UAV's cameras, a research method has been proposed for assessing spatial resolution and determining the MTF using tape and Siemens star targets. They captured images at 130 and 260 meters with an eBee fixed-wing UAV (Canon IXUS) and at 130 and 90 meters with GD-800 (Sony Nex-5N) and Phantom 4 pro multi-rotor UAVs (FC 6310). Regardless of camera type, the GSD obtained by multi-rotor and fixed-wing UAVs was nearly identical. At any flight attitude, the spatial resolution measured by the Siemens star was approximately 1 to 2 cm less than the tape target (Lee, 2019).

Cramer et al. (2020) evaluated the performance of cameras installed on advanced and conventional UAVs, such as the Phantom 4, Phantom 4 RTK, and iXM-100. In this study, the quality of image data at various levels of uncorrected, corrected original image processing, the influence of delayering, ortho-image processing, and image restoration was quantitatively evaluated. They demonstrated that image data pre-processing, as well as the acquisition, provision, and processing of reference data and additional information, are required for comparable data quality. Consequently, the Siemens star target has been utilized to assess the spatial resolution (Cramer, 2020).

Deng et al. (2020) presented a digital compressed artificial aperture (SA-DHM) holographic microscope with mechanically motionless beam scanning and optimized active deflection compensation. In this regard, the performance of the proposed method is evaluated using the Siemens star target, and the results demonstrate its potential ability to achieve an improvement in isotropic resolution. As a result, the compact beam steering system optimization proposed generates high-quality images. It has the potential to replace the conventional mechanical scanning mechanism with three significant advantages: no mechanical noise, uniform illumination with compensated scanning aberration at various angles, and a more compact system configuration (Deng, 2020).

The article is divided into five sections. Following the introduction, the second section discusses the principles of spatial resolution and the factors that influence it. The automatic spatial resolution detection process developed in this paper is then explained. The fourth section discusses the tests performed to evaluate the proposed reporting method and the results. Finally, the article's contents are summarized, and suggestions for future work are made.

2. THEORY OF SPATIAL RESOLUTION

The spatial resolution of an optical system is determined by several factors, including scene resolution, lens transparency, sensor pixel size, and the diffraction and image motion phenomena (Leung, 2013; Li, 2000; Liang, 2012; Thomas, 2008):

1. Scene resolution: it refers to the ability to see fine details in a scene and is affected by factors including ambient light, dust, and fog.
2. Lens transparency: this is determined by the resolution and measured using the Point Spread Function (PSF). The lower the PSF and image blur, the higher the lens's transparency. The transparency of a lens is determined by its quality, homogeneity, material, and lathe quality.
3. Sensor pixel size: In reality, the sampling distance is an image that, when multiplied by the image scale, yields a ground sampling distance, which is an excellent indicator of the spatial accuracy of the captured objects. In other words, the sensor's spatial resolution, also referred to as the camera's megapixel, and pixel size are identical. The image quality and level of detail that can be retrieved from the sensor improve as the pixel size of the sensor decreases, but after a certain threshold, there is no further improvement in image quality. If the pixel size is less than one limit, diffraction occurs, and as a result, the image becomes blurry and details are lost due to the behavior of light waves. In addition to the aforementioned issues, it should be noted that increasing spatial resolution increases processing time.
4. Image motion: it is the result of capturing the same point of an object in different areas of the image. The leading cause is the relative motion of the camera and the subject during the shutter's open time interval. As seen in UAV photogrammetry, image motion can be caused by a variety of factors, including camera shake, imaging of a moving object, and imaging in motion. Increase the shutter speed, move closer to the subject, and shorten the focal length to reduce image motion. Lens stabilization is an additional method for minimizing image distortion caused by camera shake. It involves rapidly shifting the lens and sensor in the opposite direction of the shake. Obviously, due to the momentary change in the principal point parameters in the interior orientation, this method is not recommended for use in photogrammetry.

2.1 Compute Spatial Resolution

The spatial resolution (GRD) is calculated using the ground pixel size (GSD) and the sensor quality index (Q), as shown in Figure 1. The Q index is determined by the pixel size (p), f-stop number (FN), and light wavelength (λ), which must be adjusted so that the Q index is close to 2.
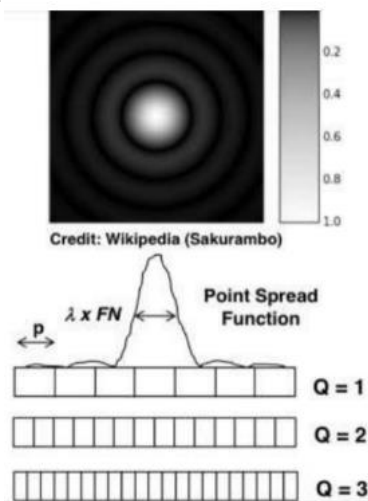

Figure 1. Shows the *Q* and GSD sensor quality indexes.

1. Spatial resolution using sensor diffraction and the Riley criterion (Equation 1):

$$GRD = 1.22 \times \frac{\lambda}{D} \times H \ , \quad (1)$$

where λ = Wavelength of Light
   D = Aperture Diameter

2. The sensor ground pixel size (Equation 2):

$$GSD = \frac{p}{L} \times H = IFOV \times H \ , \quad (2)$$

where p = Pixel Dimensions
   L = Focal Length
   IFOV = Instantaneous Field of View

3. The sensor quality index (Equation 3) and Using the Q-GSD-GRD (Equation 4):

$$Q = \frac{\lambda \times FN}{p}, FN = \frac{L}{D} \ , \quad (3)$$

$$GRD = 1.22 \times Q \times GSD \ , \quad (4)$$

where Q = Sensor Quality

According to Nyquist sampling, using Q = 2 results in the best spatial resolution. The value of Q that is chosen is an important design parameter.

2.2 Determine Spatial Resolution using Test Targets

The GRD is calculated using spatial resolution test targets, two of which are the USAF test target (Figure 2) and the Siemens test target (Figure 3).

2.2.1 USAF Test Target: Since its initial use by the United States Air Force (USAF) in 1951, this test target has undergone several modifications. Before you can fly, you must first take this target with the correct plot dimensions and position it on the ground in the direction of flight. Using horizontal and vertical lines, the spatial resolution in two flight directions and its perpendicular direction can be estimated using this information. Due to image motion, the spatial resolution in the flight direction is typically lower than that in the perpendicular direction. To avoid making the test target narrow and long, the groups of lines are spiral-arranged and each is assigned two group numbers (-8 to -3) and element numbers (1 to 6). Each group's line width and thickness are half that of the following. Compared to the previous section, the dimension of each element within each group has been reduced by 12%. Using Equation 5, spatial resolution can be expressed in terms of the number of line pairs per millimetre (LP/mm).

$$GRD\left(\frac{lp}{mm}\right) = 2^{\left(GN+ \ \frac{EN-1}{6}\right)}, \quad (5)$$
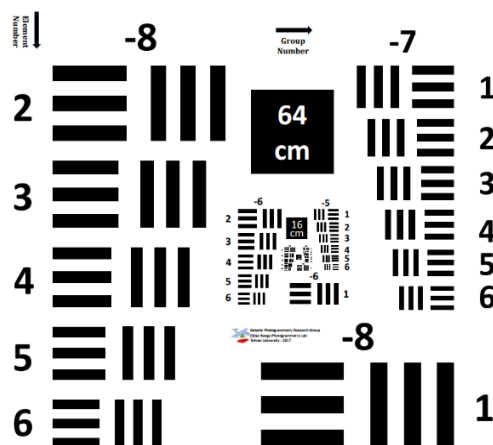
where   GN= Group Number
   EN = Element Number

Figure 2. USAF test target.

2.2.2 Siemens Test Target: The Siemens test target consists of black-and-white circle arms that become more difficult to distinguish as we move closer to the centre. Within a certain radius, the black arms blend to form a gray circle. The spatial resolution to ground pixel size ratio will be a factor of the diameter of this gray circle, which will depend on the number of arms and can be calculated using Equation 6. The Siemens test page's main advantages are its simplicity, independence from flight direction and plot scale, and high accuracy and stability in calculating spatial resolution by considering all directions. Furthermore, it directly calculates the relative amount of spatial resolution reduction regardless of flight altitude or ground pixel size.

$$\frac{GRD}{GSD} = K = \frac{\frac{D}{2}}{\sin\frac{\pi}{n}}, \quad (6)$$

where D = Diameter of the circle of ambiguity
   n = Number of target arm pairs
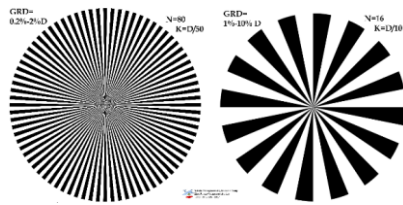
Figure 3. shows two examples of Siemens test targets used to determine the spatial resolution of aerial images.

3. MATERIALS AND METHODOLOGY

Because of the various cameras and lenses used in different types of UAVs, as well as the varying environmental conditions during imaging, the resolution of the images should be determined before each aerial imaging project, and the coefficient of decrease of the resolution image should be estimated using k. We can use the siemens target, which has black-and-white arms, to calculate the k value. In general, if we consider n black and white arms, the diameter of the circle of ambiguity on the image is measured in pixels and divided by $2/\sin(180/n)$, which if the circle of ambiguity appears as an ellipse, the most enormous diameter ellipse should be considered an instead of the circle of ambiguity's diameter. Furthermore, the Siemens target's dimensions should not be less than 15 times the GSD imaging.

According to the flowchart in Figure 4, to compare the spatial resolution of images captured by different types of multi-rotor UAVs based on the Siemens star target, images from different altitudes must be taken after designing the target and its dimensions. The coefficient of reduction of the image resolution k is then calculated based on the diameter of the circle of ambiguity using an automatic method.
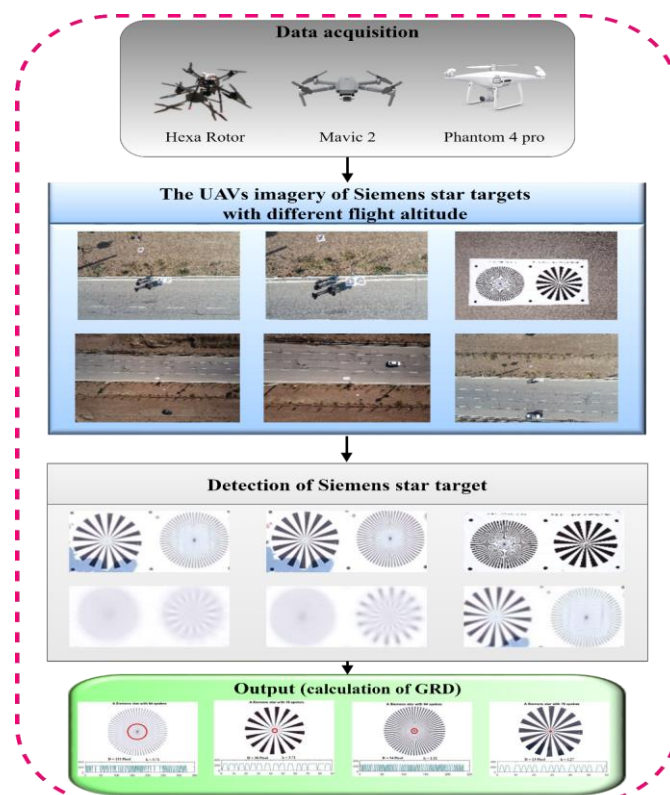
Figure 4. Flowchart of the proposed spatial resolution determination method.

According to the flowchart above, in order to calculate the spatial resolution automatically, we must first create the circle of ambiguity in the centre of the target in such a way that the other black and white arms are indistinguishable from each other after a certain radius. The necessary calculations are then performed to determine the GRD, which is explained in the section on spatial resolution, based on the diameter of the circle of ambiguity. The main idea of the proposed method for determining the spatial resolution of UAV images is captured from research (Fakhri, 2021). In research (Fakhri, 2021), the target was manually extracted from the images and the target centre was ascertained to determine the spatial resolution of the images, whereas in this research, the above steps are performed automatically. As a result, the following is the procedure for automatically calculating the above coefficient:

1. Automatic detection of the Siemens target on the image using the Template Matching method, as well as the removal of additional areas from the entire image, so that the gray values of the original image are pixel by pixel compared to the pattern image containing the identifiable target (Basulto-Lantsova, 2020).

2. Transforming the target image from RGB to Grayscale to creates a longitudinal profile of the target environment.

3. Using the Hough transform algorithm to determine the target center. Because the targets in the image may be recorded as ellipses in vertical or oblique

images, the ellipse extraction algorithm based on the Hough transform was used to fit and extract the focal center of the Siemens star target. The main advantage of using the Hough transform to fit an ellipse is that it does not require extracting the ellipse's circumferential lines (Chia, 2007).

4. Automatically drawing a circle with a radius of one pixel relative to the target's center and performing resampling operations on the circle's pixels to draw their longitudinal profile.

5. Determine the number of longitudinal profile peaks and compare them to the number of target arms utilized (if the number of target arms is less than the profile peaks, add one pixel to the radius of the drawn circle and repeat steps 4 and 5 until the number Profile peaks and arms to be equals).

4. CALCULATING THE SPATIAL RESOLUTION OF THE UAVS USED

4.1 Study Area

The spatial resolution was calculated using images captured by the UAV at different altitudes in two regions of Iran (Figure 5), including the southern part of Sakineh Paradise in Karaj city with latitude coordinates of 35.5322 and longitude 50.5244 and the western part of Taleghan city with latitude coordinates of 36.1780 and longitude 50.7681.
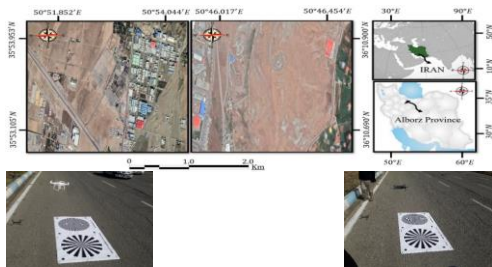

Figure 5. Study area.

4.2 UAVs

Images were acquired from new and secondhanded Phantom 4 Pro, Mavic Pro, and Hexa-rotor (with Canon-M camera) (Figure 6). These drones are controlled by a controller and are equipped with a non-metric camera, as shown in Table 1:

A. Phantom 4Pro   B. Mavic Pro   C. Hexa-rotor
Figure 6. The UAV platforms used.

Camera specifications	Phantom 4 Pro	Mavic Pro	Hexa-rotor (Canon-M)
Focal length (mm)	8.8	5	22
Effective pixel	20	12	18
Image size (pixel)	5472×3648	4000×3000	5185×3456
Sensor size (mm)	13.2×8.8	6.17×4.55	22.3×14.9

Table 1. UAVs camera specifications.

4.3 Implementation

According to the proposed method, the spatial resolution of the UAVs used to target Siemens has been conducted in two phases of operation and processing. During the operational phase, the Siemens target must first be designed and printed before being placed in the imaging scene on the ground. In this regard, the first Siemens stars with a diameter of 80 cm were intended, and in the corners of the target, circles with a diameter of 5 cm and spaced 1 meter apart were studied in the areas, as shown in Figure 7.

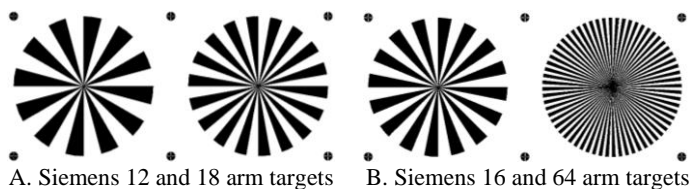A. Siemens 12 and 18 arm targets   B. Siemens 16 and 64 arm targets
Figure 7. Designed Siemens targets.

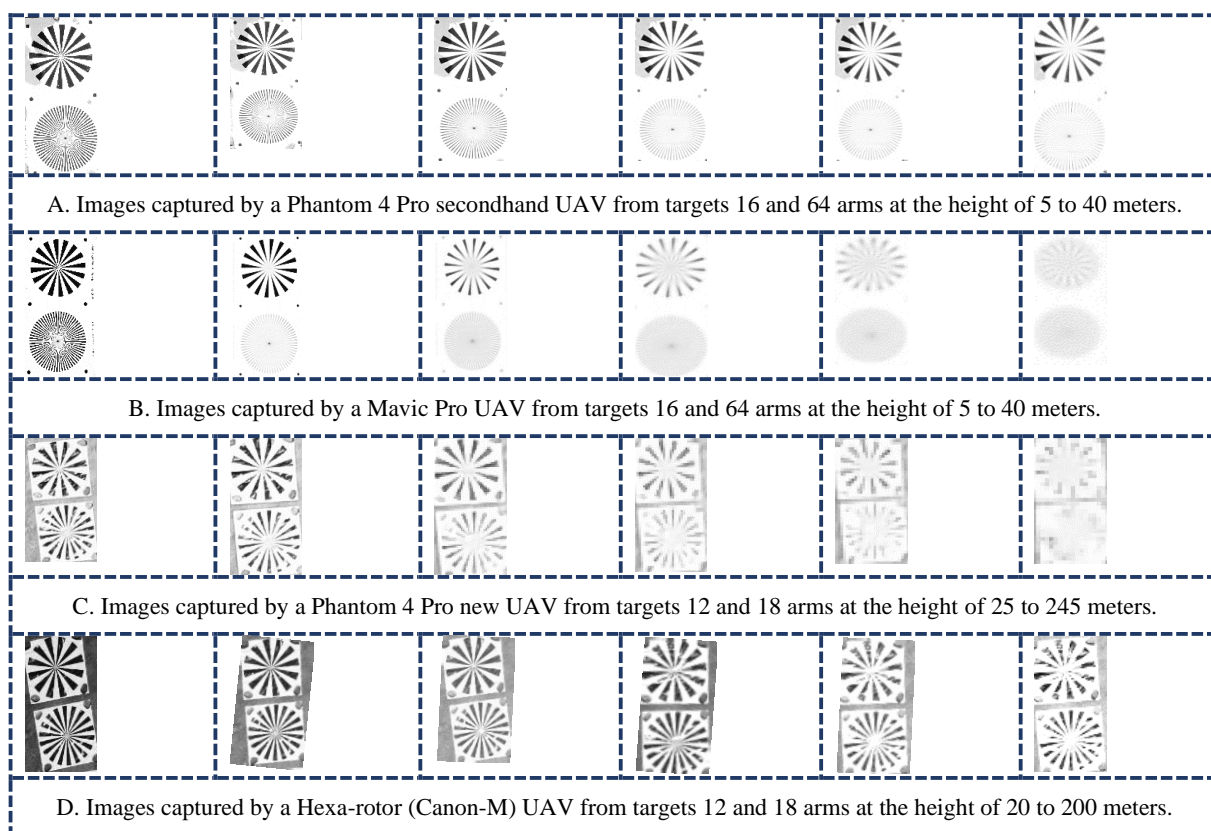The targets were imaged with UAVs after fixing the Siemens 16 and 64 arms in the Karaj area and the 12 and 18 targets in the Taleghan area. Figure 8 illustrates an example of an image captured by UAVs.

Figure 8. Shows images captured by UAVs.

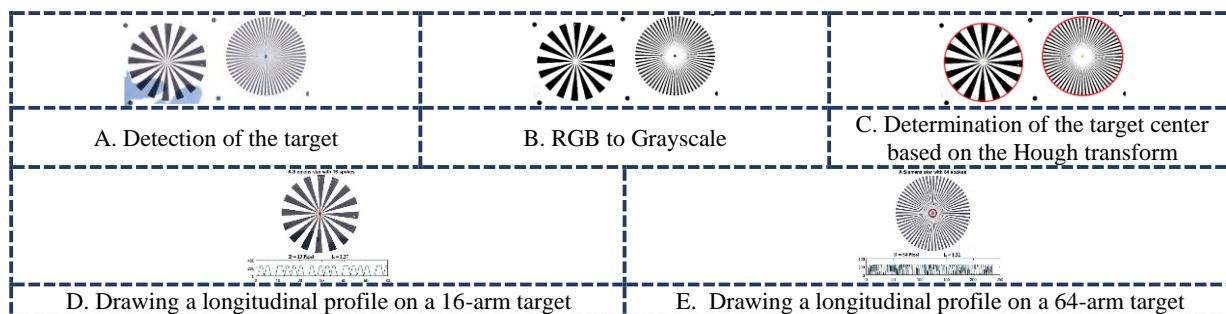The targets in the images are then automatically detected, and unnecessary areas of the image are deleted using the suggested algorithm and template matching approach, as shown in Figure 9.

A. Images captured by a Phantom 4 Pro secondhand UAV from targets 16 and 64 arms at the height of 5 to 40 meters.

B. Images captured by a Mavic Pro UAV from targets 16 and 64 arms at the height of 5 to 40 meters.

C. Images captured by a Phantom 4 Pro new UAV from targets 12 and 18 arms at the height of 25 to 245 meters.

D. Images captured by a Hexa-rotor (Canon-M) UAV from targets 12 and 18 arms at the height of 20 to 200 meters.

Figure 9. Targets detected by the proposed method and unnecessary image sections removed.

Then, to automatically detect the circle of ambiguity in the various images taken by the UAVs, after identifying the threshold and converting RGB images to Grayscale, and determining the target centre using the Hough transform technique, circles with a radius of one pixel are automatically drawn, followed by the circle profile generated using gray values 0 and 1. Figure 10 depicts an example of the algorithm's output.

A. Detection of the target

B. RGB to Grayscale

C. Determination of the target center based on the Hough transform

D. Drawing a longitudinal profile on a 16-arm target

E. Drawing a longitudinal profile on a 64-arm target

Figure 10. Shows an example of the result of the algorithm for determining spatial resolution in UAV images.

Following the application of several outputs of images captured by UAVs in the Karaj region, the spatial resolution according to Figure 11 for a secondhanded Phantom 4 Pro UAV, according to the Siemens target, 16 pairs of arms from a height of 5 to 40 meters according to the proposed method and manual method 1.28 and with the target of 64 pairs of arms has been variable around 1.31. As a result, while using the above Phantom 4 Pro secondhanded UAV, the above figure of 1.30 can be used as a spatial resolution coefficient

in computations. Furthermore, the spatial resolution in the Mavic Pro UAV based on the Siemens target is 16 pairs of arms from a height of 5 to 60 meters, according to the proposed technique and the manual method, is equivalent to 3.71. With the target of 64 pairs of arms is approximately 3.68. As a result, when using the Mavic Pro UAV, the value of 3.70 can be used as a spatial resolution coefficient in the computations.
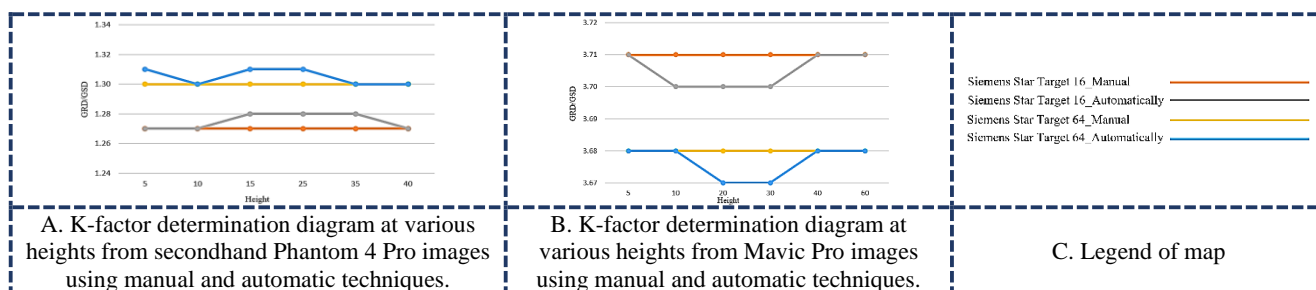

A. K-factor determination diagram at various heights from secondhand Phantom 4 Pro images using manual and automatic techniques.	B. K-factor determination diagram at various heights from Mavic Pro images using manual and automatic techniques.	C. Legend of map

Figure 11. Calculation of the spatial resolution coefficient.

According to Figure 12, the spatial resolution of the images captured by the new Phantom 4 Pro for the Siemens target, is 12 pairs of arms from the Taleghan region and at an altitude of 25 to 245 meters, a value equal to 1.16, and with the target of 18 pairs of arms, it varies around 1.22. Based on this, the value of 1.2 can be used as a spatial resolution coefficient in the calculations for using the new Phantom 4 Pro UAV. Based on the proposed technique and manual method, the

spatial resolution of the images captured by the Hexa-rotor UAV with Canon-M camera for the Siemens target is 12 pairs of arms at an altitude of 20 to 200 meters, a value equal to 1.20. With a target of 18 pairs of arms, it varies around 1.16. As a result, when calculating the spatial resolution coefficient for the Hexa-rotor UAV with the Canon-M camera, the value of 1.2 can be used.
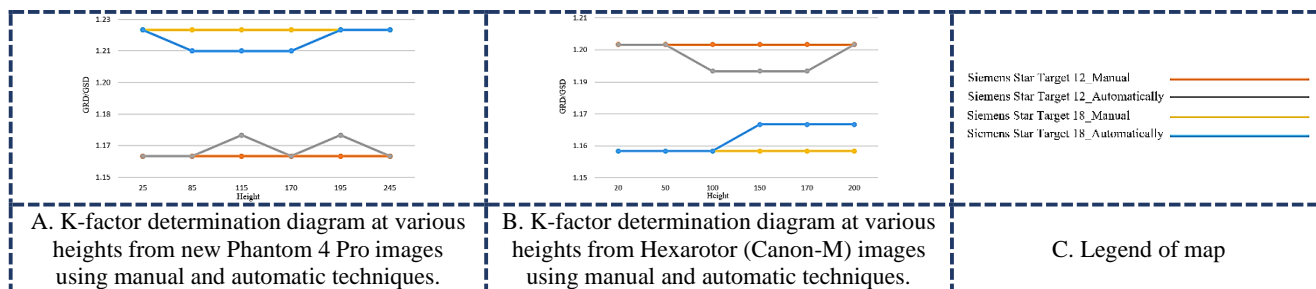

A. K-factor determination diagram at various heights from new Phantom 4 Pro images using manual and automatic techniques.	B. K-factor determination diagram at various heights from Hexarotor (Canon-M) images using manual and automatic techniques.	C. Legend of map

Figure 12. Calculation of the spatial resolution coefficient.

5. CONCLUSION

Due to the variety of cameras used in different types of UAVs and the impact of lens resolution on the quality of spatial data extracted from UAV images, the image resolution of the camera used in the UAV photogrammetry system must be determined prior to imaging and used to determine GSD images. Since the lens resolution varies between imaging projects, it is crucial to define the image resolution for each flight by selecting a coefficient based on camera specifications, flight altitude, area coverage and GSD. As a result, the Siemens star target is an important method for determining spatial resolution. According to the results, the Siemens star target has a greater coefficient of spatial resolution loss in the direction of blur and the platform movement than orthogonal targets, and its efficiency is higher. Moreover, analysing the imaging data presented under various conditions shows that increasing the imaging distance, which corresponds to increasing the UAV's flying altitude, gradually increases the coefficient k. According to the author's observations, the k-factor increases in a variety of weather conditions, including low light, sunset, air and

dust pollution, severe camera vibrations, sensor life and as such.

REFERENCES

Azimi, S., Mokhtarzade, M., Zoej, M.J.V., 2013. Spatial Resolution Measurement of UltraCamd Images Using Siemens Star Print. Geospatial Engineering Journal, 4(4), 13-24 .

Basulto-Lantsova, A., Padilla-Medina, J.A., Perez-Pinal, F.J., Barranco-Gutierrez, A.I., 2020: Performance comparative of OpenCV Template Matching method on Jetson TX2 and Jetson Nano developer kits. 2020 10th Annual Computing and Communication Workshop and Conference (CCWC) ,

Chia, A.Y.S., Leung, M.K., Eng, H.-L., Rahardja, S., 2007: Ellipse detection with hough transform in one dimensional parametric space. 2007 IEEE International Conference on Image Processing ,

Cramer, M., Zhang, S., Meibner, H., Reulke, R., 2020. Quality assessment of high-resolution UAV imagery and products. Proceedings of the 40. Wissenschaftlich-Technische Jahrestagung der DGPF in Stuttgart, Stuttgart, Germany, 4-6 .

Cryderman, C., Mah, S.B., Shufletoski, A., 2014. Evaluation of UAV photogrammetric accuracy for mapping and earthworks computations. Geomatica, 68(4), 309-317 .

Deng, Y., Huang, C.-H., Vinoth, B., Chu, D., Lai, X.-J., Cheng, C.-J., 2020. A compact synthetic aperture digital holographic microscope with mechanical movement-free beam scanning and optimized active aberration compensation for isotropic resolution enhancement. Optics and Lasers in Engineering, 134, 106251 .

Fakhri, S.A., Latifi, H., 2021. A Consumer Grade UAV-Based Framework to Estimate Structural Attributes of Coppice and High Oak Forest Stands in Semi-Arid Regions. Remote Sensing, 13(21), 4367 .

Fakhri, S.A., Fakhri, S.A., Saadatseresht, M., 2019: ROAD CRACK DETECTION USING GAUSSIAN/PREWITT FILTER. International Archives of the Photogrammetry, Remote Sensing & Spatial Information Sciences.

Fakhri, S.A., Saadatseresht, M., Varshosaz, M., Zakeri, H., 2021. Automatic Estimation of the Spatial Resolution Coefficient of UAV Images Based on Siemens Star Target [Research]. Journal of Geomatics Science and Technology, 10(4), 191-204. http://jgst.issge.ir/article-1-949-en.html

Fakhri, S.A., Saadatseresht, M., Varshosaz, M., Zakeri, H., 2022: Evaluation of UAV Photogrammetric capability in Road Pavement Cracks Detection. Amirkabir Journal of Civil Engineering, 54(5), 4-4. https://doi.org/10.22060/ceej.2021.19815.7263

Kangas, A., Gobakken, T., Puliti, S., Hauglin, M., Naesset, E., 2018. Value of airborne laser scanning and digital aerial photogrammetry data in forest decision making. Silva Fennica .19, (1)52,

Lee, J.-O., Sung, S.-M., 2019. Quality Evaluation of UAV Images Using Resolution Target. 22(1), 103-113 .

Lee, J., Sung, S., 2016. Evaluating spatial resolution for quality assurance of UAV images. 24(2), 141-154 .

Leung, T.S., Jiang, S., 2013. Acousto-optic imaging of a color picture hidden behind a scattering layer. Optics Express, 21(22), 26780-26785 .

Li, J., 2000. Spatial quality evaluation of fusion of different resolution images. International Archives of Photogrammetry and Remote Sensing, 33(B2; PART 2), 339-346 .

Liang, S., Wang, J., Jiang, B., 2012. A systematic view of remote sensing. Advanced remote sensing, 1-31 .

Lim, P.-C., Son, J., Kim, T., 2019. Development and Comparative Analysis of Mapping Quality Prediction Technology Using Orientation Parameters Processed in UAV Software. 35(6_1), 895-905 .

Mohammadi, M., Rashidi, M., Mousavi, V., Karami, A., Yu, Y., Samali, B., 2021. Quality evaluation of digital twins generated based on UAV photogrammetry and TLS: Bridge case study. Remote Sensing, 13(17), 3499.

Motayyeb, S., Fakhri, S.A., Varshosaz, M., Pirasteh, S., 2022: ENHANCING CONTRAST OF IMAGES TO IMPROVE GEOMETRIC ACCURACY OF A UAV PHOTOGRAMMETRY PROJECT. The International Archives of Photogrammetry, Remote Sensing and Spatial Information Sciences, 43, 389-398 .

Mousavi, V., Varshosaz, M., Remondino, F., 2021a. Evaluating tie points distribution, multiplicity and number on the accuracy of uav photogrammetry blocks. The International Archives of Photogrammetry, Remote Sensing and Spatial Information Sciences, 43, 39-46.

Mousavi, V., Varshosaz, M., Remondino, F., 2021b. Using Information Content to Select Keypoints for UAV Image Matching. Remote Sensing, 13(7), 1302.

Park, J.K., Jung, K.Y., 2021. Accuracy evaluation of earthwork volume calculation according to terrain model generation method. Journal of the Korean Society of Surveying, Geodesy, Photogrammetry and Cartography, 39(1), 47-54 .

Saadatseresht, M., Hashempour, A., Hasanlou, M., 2015. UAV photogrammetry: a practical solution for challenging mapping projects. The International Archives of Photogrammetry, Remote Sensing and Spatial Information Sciences, 40(1), 619 .

Thomas, C., Ranchin, T., Wald, L., Chanussot, J., 2008. Synthesis of multispectral images to high spatial resolution: a critical review of fusion methods based on remote sensing physics. IEEE Transactions on Geoscience and Remote Sensing, 46(5), 1301-1312. https://doi.org/10.1109/tgrs.2007.912448

Yang, B., Ali, F., Yin, P., Yang, T., Yu, Y., Li, S., Liu, X., 2021. Approaches for exploration of improving multi-slice mapping via forwarding intersection based on images of UAV oblique photogrammetry. Computers & Electrical Engineering, 92, 107135 .

Yu, H., Fu, J., Zhou, C., Song, X., Chen, H., 2022: A Review of UAV Tilt Photogrammetry Technology for Digital Modeling of Hydropower Station Geomorphology. Proceedings of 2021 Chinese Intelligent Systems Conference